Bioorganic & Medicinal Chemistry 19 (2011) 1535–1540

Contents lists available at ScienceDirect

Bioorganic & Medicinal Chemistry

journal homepage: www.elsevier.com/locate/bmc

# LC–MS and NMR characterization of the purple chromophore formed in the *o*-aminobenzaldehyde assay of dihydrodipicolinate synthase

Voula Mitsakos [a,b], Sean R. A. Devenish [c,†], Paul A. O'Donnell [b], Juliet A. Gerrard [c], Craig A. Hutton [a,b,*]

[a] School of Chemistry, The University of Melbourne, Victoria 3010, Australia
[b] Bio21 Molecular Science and Biotechnology Institute, The University of Melbourne, Victoria 3010, Australia
[c] Biomolecular Interaction Centre and School of Biological Sciences, University of Canterbury, Christchurch, New Zealand

ARTICLE INFO

*Article history:*
Received 16 November 2010
Revised 3 December 2010
Accepted 13 December 2010
Available online 16 December 2010

*Keywords:*
Dihydrodipicolinate synthase
*o*-Aminobenzaldehyde
Purple chromophore
Enzyme assay
Lysine biosynthesis

ABSTRACT

The enzyme dihydrodipicolinate synthase (DHDPS) has been widely investigated as a target for new antibiotics. The *o*-aminobenzaldehyde (*o*-ABA) assay is routinely used as a highly specific, if qualitative, tool for DHDPS purification, whereby fractions containing active DHDPS appear purple upon addition of *o*-ABA. The purple adduct absorbs in the visible region (540 nm) but has never been characterized in the 50 years since it was first reported. Structural characterization of this purple compound has been performed by UV spectrophotometry, NMR spectroscopy and tandem mass spectrometry. The extinction coefficient of this chromophore was also determined.



## 1. Introduction

The first committed step in the diaminopimelate (DAP) biosynthetic pathway is catalyzed by the homotetrameric enzyme dihydrodipicolinate synthase (DHDPS), which belongs to the *N*-acetylneuraminate lyase (NAL) family of enzymes.[1] The reaction catalyzed by DHDPS is the condensation of aspartate semi-aldehyde (*S*)-(ASA) **1** and pyruvate **2** to give HTPA [(2*S*,4*S*)-4-hydroxy-2,3,4,5-tetrahydrodipicolinate **3**, Fig. 1].[2] HTPA was previously thought to afford (2*S*)-2,3-dihydrodipicolinate (DHDP **4**) via spontaneous dehydration, but recent studies have found that HTPA **3** is itself the substrate of the next enzyme in the pathway, dihydrodipicolinate reductase (DHDPR).[3]

The DAP pathway provides the essential amino acid lysine and its immediate precursor *meso*-DAP, both of which are major constituents of the bacterial peptidoglycan cell wall. Lysine is a constituent of the cell wall in Gram-positive bacteria (for example, the pathogenic bacterium *Staphylococcus aureus*) while the cell wall of Gram-negative bacteria such as *Escherichia coli* contains *meso*-DAP.[4] Inhibitors of the DAP pathway are being investigated as a potential new class of antibiotics.[5–10]

Two assays commonly employed to measure the activity of DHDPS are the coupled assay and the *o*-aminobenzaldehyde (*o*-ABA) assay. The DHDPS–DHDPR coupled assay is commonly used to determine accurate kinetic data for DHDPS.[11,12] The oxidation of NADPH to $NADP^+$ catalyzed by DHDPR is monitored at 340 nm (Fig. 2A) to provide an indirect measure of the initial rate of DHDPS. The main drawbacks of this assay are the need to purify the coupling enzyme DHDPR, which is required in large excess with respect to DHDPS, and care must always be taken to ensure the measured rate is proportional to the amount of DHDPS used. Furthermore, for DHDPS inhibitor screening, the coupled assay may result in false positives if the assayed compound is an inhibitor of DHDPR.

The *o*-ABA assay is a qualitative method that is the assay of choice for DHDPS purification. The DHDPS product reacts with *o*-ABA **5** under acidic conditions to form a purple chromophore that is monitored at 540 nm (Fig. 2B).[13] The identity of this chromogenic compound has not been determined, despite the assay having been used since the late 1940s. Schöpf and co-workers demonstrated that *o*-ABA **5** reacts with pyrrolines and piperidines to generate yellow-orange dihydroquinazolinium adducts.[14,15] In agreement with these observations, Vogel and Davis[16] report a yellow-colored dihydroquinazolinium compound when *o*-ABA **5** reacts with $\Delta^1$-pyrroline **6a** and Larson et al.[17] reveal that condensation of *o*-ABA **5** with $\Delta^1$-piperidine-6-carboxylic acid leads to an orange-colored dihydroquinazolinium derivative. Generation of the proposed adducts in the aforementioned studies presumably entails 1,2-addition of *o*-ABA **5** to the $\Delta^1$-pyrroline **6a** or $\Delta^1$-piperidine **6b** to generate an aminal **7** (Scheme 1).[14,15] Condensation of the endocyclic nitrogen with the aldehyde then generates, after

* Corresponding author. Tel.: +61 3 8344 2393; fax: +61 3 9347 8124.
*E-mail address:* chutton@unimelb.edu.au (C.A. Hutton).
† Present address: Department of Biochemistry, University of Cambridge, Cambridge, UK.

0968-0896/$ - see front matter © 2011 Elsevier Ltd. All rights reserved.
doi:10.1016/j.bmc.2010.12.029

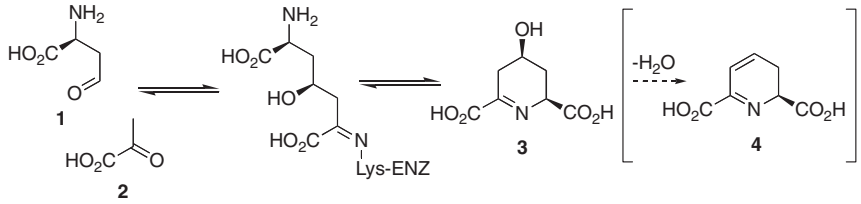


**Figure 1.** The reaction catalyzed by DHDPS to yield HTPA **3**.

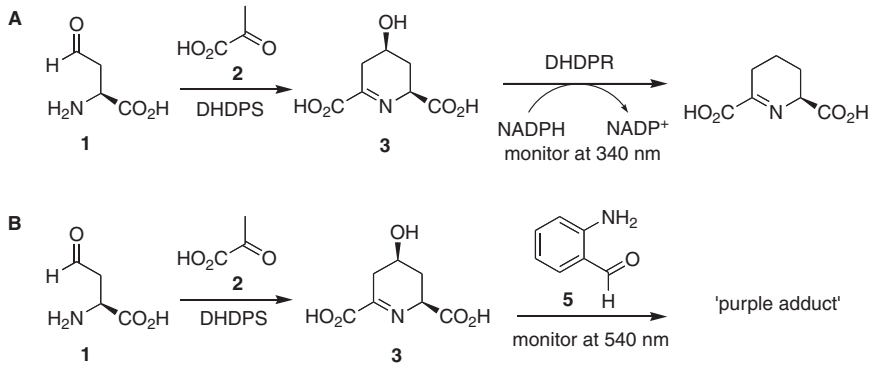


**Figure 2.** (A) Coupled assay (DHDPS–DHDPR), and (B) *o*-aminobenzaldehyde (*o*-ABA) assay.

dehydration, the dihydroquinazolinium species **9**. Furthermore, reaction of reduced pyridine nucleotides with *o*-ABA **5** has been reported to produce an orange colored adduct under acidic conditions, with maximum color development occurring over a 30–60 min interval.[18]

Yugari and Gilvarg showed that the unstable product of the DHDPS-catalyzed reaction reacts with *o*-ABA **5** to give a purple adduct.[13] The reaction has a lag followed by slow formation of the purple chromophore, which is accelerated by the addition of acid. Yamakura et al. showed that *o*-ABA adduct formation is linearly related to the amount of the product of the DHDPS-catalyzed reaction.[19] Formation of the purple adduct allows the *o*-ABA assay to be used for qualitative purposes; for example, visually identifying protein purification fractions containing active DHDPS enzyme. For decades, investigators who have worked with DHDPS have been keen to elucidate the structure of this purple chromophore. We report here the first characterization of this compound. In addition, the value of the extinction coefficient for the chromophore was determined, enabling the *o*-ABA assay to be utilized in a more quantitative manner.

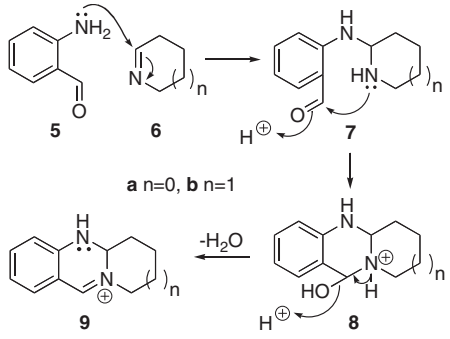


**Scheme 1.** 1,2-Addition of *o*-ABA **5** with pyrrolines **6a** and piperidines **6b** to generate dihydroquinazolinium species **9**.

## 2. Experimental methods

### 2.1. Chemical reagents, substrate and enzyme

All chemicals were of the highest grade and were purchased from Sigma–Aldrich unless otherwise stated. HPLC-grade water and acetonitrile were obtained from Burdick & Jackson. (*S*)-ASA **1** was prepared as described previously.[20] *E. coli* DHDPS was prepared as a His-tagged construct, as described previously.[21]

### 2.2. *o*-ABA assay

Formation of the purple chromophore was monitored by UV–vis spectrophotometry (Varian Cary 50 Bio). The enzymatic mixture contained 175 μL of buffer (500 mM Tris–HCl, pH 8.0), 50 μL pyruvate 2 (20 mM in water), 10 μL (*S*)-ASA **1** (100 mM in water) and 10 μL *E. coli* DHDPS (100 μg/mL) made up to a volume of 700 μL with $H_2O$. The enzymatic reaction was allowed to proceed for 10 min before being quenched with 175 μL acid (2 M HCl). One-hundred and twenty five microliters of *o*-ABA **5** was added (17 mM in water) to a final volume of 1 mL. Formation of the purple chromophore was monitored over 60 min, with samples collected at 10, 30 and 60 min for MS analysis.

### 2.3. ESI-TOF mass spectrometry

LC–MS experiments were performed on an Agilent 6510 Q-TOF LC/MS Mass Spectrometer coupled to an Agilent 1100 LC system (Agilent, Palo Alto, CA). All data were acquired and reference mass corrected via a dual-spray electrospray ionization (ESI) source. Each scan or data point on the Total Ion Chromatogram (TIC) is an average of 10,000 transients, producing a scan every second. TOF spectra were created by averaging the scans across each peak. Typical MS conditions were: ionization mode: ESI, positive mode; drying gas flow: 7 L/min; nebulizer: 30 psi; drying gas temperature: 325 °C; Vcap: 4 kV; fragmentor: 150 V; skimmer: 65 V; Octopole RF peak: 750 V. The Agilent HPLC system employed a

C18 (Agilent 300SB) 2.1 mm × 75 mm reversed-phase column. Elution was carried out using a water/acetonitrile gradient in the presence of 0.1% formic acid at a flow rate of 250 μL/min. In source fragmentation of the parent ion (LC–MS/MS) was at a voltage of 150 V and fragmentation of the abundant daughter fragment (LC–MS/MS/MS) was performed at a voltage of 400 V.

UV–vis–LC–MS analyses were performed on an Agilent 6520 Accurate-Mass Q-TOF LC/MS Mass Spectrometer with an Agilent 1200 Series Diode array detector (G1315C). The Agilent HPLC system employed a C18 (Agilent XDB) 2.1 mm × 50 mm (1.8 μm) column. Data acquisition, LC and MS conditions were the same as for the Agilent 6510 Q-TOF LC/MS instrument.

### 2.4. NMR spectroscopy

NMR spectra were obtained on a Varian INOVA spectrometer, operating at 500 MHz for $^{1}H$ and 125 MHz for $^{13}C$ detection. Spectra obtained in $H_2O$ were locked and shimmed on a $D_2O$ insert and run using presaturation with a satpwr of 20, satdly of 3.0 s, gain of 24 and a d1 of 0 s to reduce the intensity of the water signal. All spectra were referenced to the methyl resonance of added *t*-butanol at $\delta$ 1.24 ppm for $^{1}H$, and 30.29 ppm for $^{13}C$. The purple chromophore was prepared in a 5 mm NMR tube containing 500 μL of buffer (200 mM $NaP_i$, pH 8.0), 400 μL ASA (100 mM in water), 100 μL pyruvate (400 mM in water), 100 μL *o*-ABA (400 mM in ethanol) and 100 μL *E. coli* DHDPS (1 mg/mL). Reaction progress was monitored by $^{1}H$ NMR, and when complete the sample was dried under a stream of nitrogen and re-dissolved in $D_2O$ for characterisation.

### 2.5. Extinction coefficient

The extinction coefficient of the purple chromophore was determined indirectly. With the aforementioned *o*-ABA assay, the enzyme mixture was incubated at 37 °C for 10, 20, 30 and 40 min, followed by addition of *o*-ABA **1** and acid and monitoring of the formation of the chromophore over 70 min. The enzyme incubation period was varied in order to deduce the time required for complete consumption of substrates (*S*)-ASA **1** and pyruvate **2**.

## 3. Results and discussion

### 3.1. UV spectrophotometry and LC–MS

The DHDPS *o*-ABA assay was performed with formation of the purple adduct monitored by UV–vis spectrophotometry at 540 nm (see Supplementary data). The enzymatic reaction was allowed to proceed for 10–40 min to accumulate the DHDPS reaction product HTPA **3**. Upon addition of acid and *o*-ABA **1**, the reaction with HTPA **3** was allowed to proceed for 70 min. The absorbance at 540 nm was found to increase over 60 min (Fig. 3). Samples were collected at 10, 30 and 60 min time intervals post-addition of *o*-ABA **5** for LC–MS analysis.

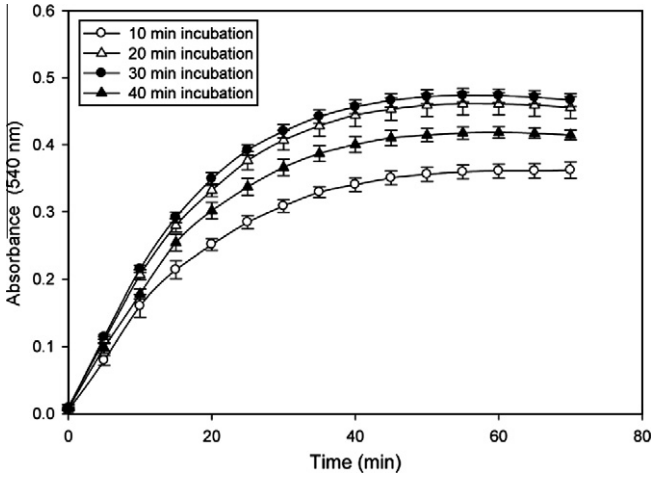


**Figure 3.** Formation of purple adduct monitored by UV–vis spectrophotometry at 540 nm. Data points are the arithmetic mean ($n = 3$) ±SEM.

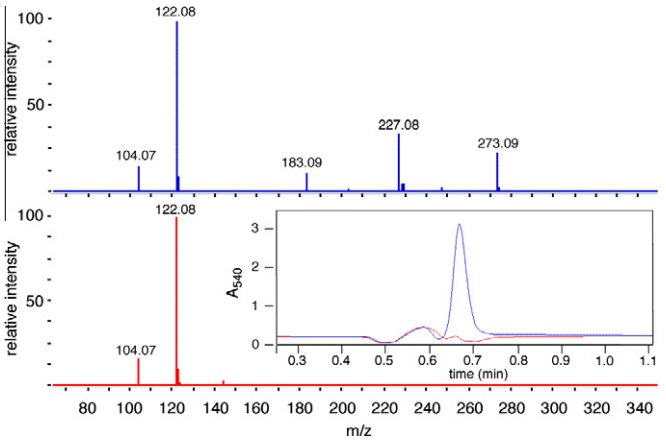


**Figure 4.** UV–vis–LC–MS analysis of sample following 10 min enzyme incubation and 60 min *o*-ABA reaction. Top: MS of fraction absorbing at 540 nm, eluting at ~0.7 min. Bottom: MS of control sample with no enzyme added (reference ion at 122.08). Inset; HPLC monitored at 540 nm, showing peak eluting at ~0.7 min (blue), control sample with no enzyme added (red).

LC–MS analysis of the *o*-ABA assay mixture was performed with concurrent detection of absorbance at 540 nm (Fig. 4 inset). A compound eluted at ~0.7 min with a strong absorbance at 540 nm in both the 30 and 60 min post-*o*-ABA incubation samples (10 min enzyme incubation). This fraction was subjected to MS analysis (Fig. 4).

Analysis of the fraction absorbing at 540 nm shows a molecular ion at *m/z* 273.09, with only very weak intensity ions observed at *m/z* >273 (Fig. 4). The control sample (no enzyme) shows no absorbance peak at 0.7 min and no MS peak at *m/z* 273, indicating that the compound that absorbs at 540 nm has a molecular weight of 273 and is formed by reaction of *o*-ABA with the enzymatic reaction product. Further, time-dependent LC–MS analysis revealed that the *m/z* 273 peak increased in intensity over 60 min, in accordance with the increase in absorbance at 540 nm over this time. Accurate mass measurement revealed a molecular weight of 273.08675, corresponding to a molecular formula of $C_{14}H_{12}N_2O_4$, which is consistent with the condensation of HTPA **3** and *o*-ABA **5** with the loss of two molecules of water (see Supplementary data).

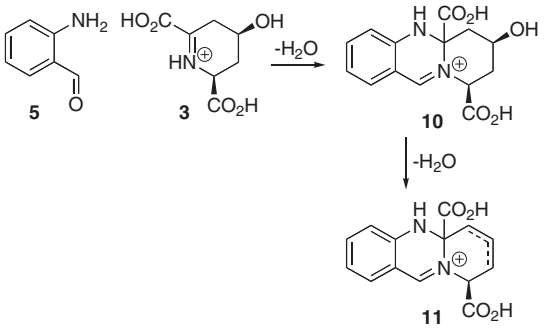


**Scheme 2.** Possible route to purple adduct from *o*-ABA **5** and HTPA **3** via 1,2-addition/condensation/dehydration to generate dihydroquinazolinium adduct **11**.

Formation of the purple chromophore was initially postulated to occur through addition of the amine of *o*-ABA **5** to the imine of HTPA **3** (Scheme 2), analogous to the postulated reaction of *o*-ABA **5** with piperidines **6b** to generate colored adducts (vide supra, Scheme 1). This reaction would generate dihydroquinazolinium adduct **10**. Compound **10** could subsequently lose water to give the adduct **11** in order to generate a molecule of the established molecular formula; however, the driving force for such a dehydration is not obvious.

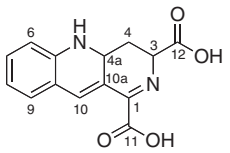


12

**Figure 6.** Structure and numbering of the purple adduct **12**.

### 3.2. NMR spectroscopy

To further characterize the purple chromophore, the *o*-ABA assay mixture was analyzed by NMR spectroscopy. The purple adduct was prepared by combining the assay constituents in an NMR tube. The reaction progress was monitored by $^1$H NMR spectroscopy, and when complete the sample was dried under a stream of nitrogen and re-dissolved in $D_2O$ for further characterization.

The $^1$H NMR spectrum of the assay mixture suggested that the crude product was sufficiently pure to allow structure elucidation (Fig. 5). The $^1$H NMR spectrum reveals aromatic resonances at $\delta$ 6.6–7.6 with two doublets and two triplets indicating an *ortho*-substituted aromatic ring. A singlet at $\delta$ 7.6 is characteristic of an isolated aromatic/vinylic proton. Two resonances at $\delta \sim$4.6 (d and dd) correspond to methine CHs adjacent to electronegative atoms (O or N), and two upfield resonances at $\delta$ 2.2–2.6 (dt and dd) are consistent with geminal protons. Together, the aliphatic resonances are consistent with an ABMX-type system. This pattern of resonances does not match that expected from **11**, which should give rise to three vinylic resonances and three aliphatic resonances.

Reassessment of the structure of the adduct in line with the NMR data led to postulation of the diazaanthracene structure **12** (Fig. 6). This compound possesses a single, isolated vinylic proton together with a $CHCH_2CH$ system of aliphatic protons, in accord with the NMR data. The resonances at $\delta \sim$4.6 correspond to methine CHs at C3 and C4a while the upfield resonances at $\delta$ 2.2–2.6 correspond to the geminal protons at C4. Further, the singlet at $\delta$ 7.6 corresponds to the vinylic proton at C10 and the two doublets and two triplets at $\delta$ 6.6–7.6 correspond to the aromatic protons on C6–C9.

In addition to the 1D $^1$H NMR data described above, 2D NMR spectroscopic analysis was undertaken, with Correlation Spectroscopy (COSY), Heteronuclear Single Quantum Correlation (HSQC) and Heteronuclear Multiple-Bond Correlation (HMBC) experiments run on the crude purple adduct (see Supplementary data). The aromatic ring of the *o*-ABA-derived moiety was easily identifiable, with quaternary carbon shifts being obtained from HMBC correlations. Likewise, the coupled aliphatic system could be clearly discerned in the COSY spectrum, with the two downfield protons at $\delta$ 4.59 and 4.51 ppm coupled to the geminal protons at $\delta$ 2.20 and 2.56 ppm. The singlet at $\delta$ 7.58 ppm showed no COSY correlations, but did show HMBC correlations to carbon atoms in both the aromatic ring and the HTPA-derived ring, consistent with the proposed structure **12**. 1D $^1$H and $^{13}$C NMR data are listed in Table 1, with COSY and HMBC correlations shown in Table 2. Importantly, the proton spectra obtained before and after the 2D experiments were not significantly different from that obtained during observation of formation of the chromophore in $H_2O$ (see Supplementary data), indicating the compound had not degraded during drying or data acquisition.

The proposed structure is consistent with nucleophilic attack of the *o*-ABA nitrogen at C4 of HTPA **3** (C4a in **12**) with substitution of the hydroxyl group. Imine–enamine tautomerization would generate enamine **14** and subsequent condensation with the aldehyde group of *o*-ABA **5** would furnish diazaanthracene **12** (Scheme 3). An alternative mechanism for the formation of adduct **12** would be through 1,4-addition of the amine of *o*-ABA **5** to DHDP **4**; however, in these and our recent studies no evidence for the spontaneous formation of DHDP **4** from HTPA **3** was observed.[3]

Further analysis of the NMR data suggests that only one of two possible diastereoisomers of adduct **12** is formed. The C4a proton exhibits one small and one large coupling (dd, $J$ = 4.5, 11.9 Hz), consistent with *gauche* and antiperiplanar relationships to the C4 protons, indicating the C4a proton is pseudo-axial. The C3 proton shows just a small coupling (d, 4.7 Hz). The absence of any large coupling between the C3 and C4 protons indicates the C3 proton

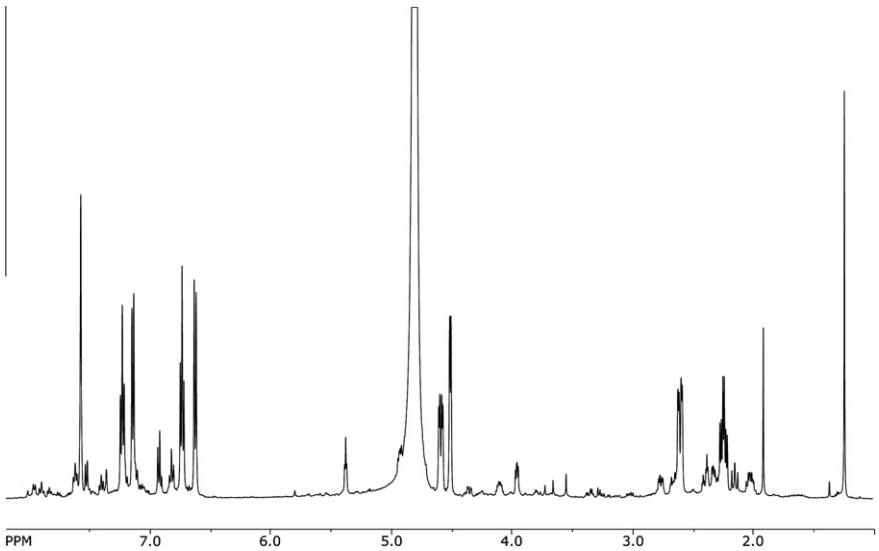


**Figure 5.** $^1$H NMR spectrum of the purple adduct obtained in $D_2O$.

**Table 1**
$^{1}H$ and $^{13}C$ NMR data for purple adduct

| Position | $^{13}C$ $\delta$[a] ($D_2O$) | $^{1}H$ $\delta$ ($D_2O$) | Multiplicity | $J$ (Hz) |
|---|---|---|---|---|
| 1 | 167.3 | | | |
| 3 | 58.4 | 4.51 | d | 4.7 |
| 4 | 29.6 | | | |
| 4a | 47.0 | 4.59 | dd | 4.5, 11.9 |
| 4α | | 2.60 | dd | 4.8, 13.1 |
| 4β | | 2.24 | dt | 5.7, 12.7 |
| 5a | 149.2 | | | |
| 6 | 115.2 | 6.63 | d | 8.1 |
| 7 | 135.9 | 7.24 | t | 7.7 |
| 8 | 120.4 | 6.74 | t | 7.4 |
| 9 | 132.3 | 7.15 | d | 7.6 |
| 9a | 121.3 | | | |
| 10 | 146.2 | 7.58 | s | |
| 10a | 118.3 | | | |
| 11 | 170.4 | | | |
| 12 | 175.6 | | | |

[a] $^{13}C$ chemical shifts were obtained indirectly from the HSQC and HMBC experiments.

**Table 2**
COSY and HMBC correlations observed for the purple adduct **12**

| Proton | COSY | HMBC |
|---|---|---|
| H3 | H4β | C1, C4, C4a, (C11), C12 |
| H4a | H4α, H4β | C4, (C10), C10a |
| H4α | H4a, H4β | (C3), C4a, C10a, (C12) |
| H4β | H3, H4a, H4α | C3, C4a, (C10), C12 |
| H6 | H7 | C8, C9a |
| H7 | H6, H8 | C5a, C9 |
| H8 | H7, H9 | C6, C9a |
| H9 | H8 | C5a, C7, C10 |
| H10 | | C1, C4a, C5a, C9, (C9a) |

Bracketed values indicate weak correlations.

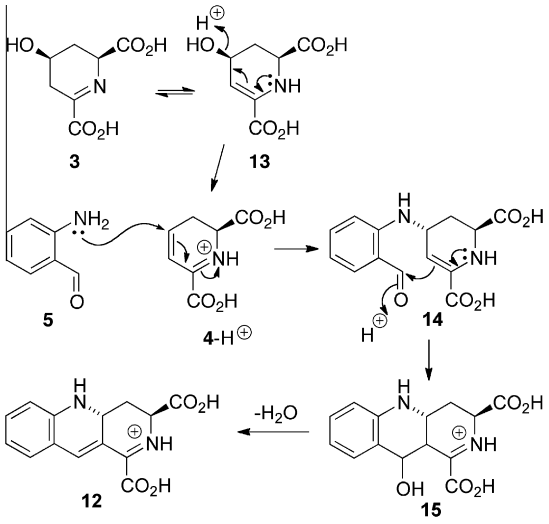


**Scheme 3.** Proposed mechanism of formation of putative purple adduct **12** from *o*-ABA **5** and HTPA **3**.

is pseudo-equatorial. Accordingly, the C3 and C4a protons of **12** must be positioned on opposite sides of the ring. In HTPA **3** the corresponding protons are on the same side of the ring, thus indicating inversion has occurred during the reaction of HTPA **3** with *o*-ABA **5**. Direct $S_N2$ displacement of a secondary hydroxyl group, either of HTPA **3** or its enamine tautomer **13**, by the *o*-ABA amine does not appear to be a favorable process. Accordingly, we postulate that loss of the hydroxyl group from **13** under acidic conditions generates protonated DHDP **4**, which then undergoes preferential axial attack by *o*-ABA from the face opposite the carboxyl group to generate **14** (Scheme 3). The formation of protonated DHDP may be assisted by *o*-ABA as previous findings infer that DHDP **4** is not a product of the DHDPS-catalyzed reaction.[2,3] Subsequent intramolecular attack of the enamine group of **14** onto the aldehyde, followed by dehydration, then generates the adduct **12**.

### 3.3. $MS^2$ analysis

Further evidence for the structure of the adduct **12** was sought through more detailed mass spectrometric analysis. The molecular ion at *m/z* 273.09 was subjected to $MS^2$ analysis, yielding daughter ions at *m/z* 157.08 (47%), 183.09 (14%), 155.06 (11%), 211.09 (8%), 130.06 (5%), 229.10 (5%) and 227.08 (2%), corresponding to losses of $C_4H_4O_4$, $C_2H_2O_4$, $C_4H_6O_4$, $CH_2O_3$, $C_5H_5NO_4$, $CO_2$ and $CH_2O_2$, respectively (Fig. 7).

The formation of the predominant daughter ion at *m/z* 157.08 is consistent with a retro Diels–Alder reaction to lose acrylic acid ($-C_3H_4O_2$) and decarboxylation ($-CO_2$) (Fig. 8). The 1,2-adduct **11** contains a quaternary centre and as such a retro Diels–Alder reaction is impossible. The formation of the daughter ion at *m/z* 227.08 is attributed to a concerted loss of $[CO_2+H_2]$ (Fig. 8). The formation of the daughter ions at *m/z* 229.10 and 211.09 is attributed to loss of $CO_2$ and $[CO_2+H_2O]$, respectively. The daughter ion at *m/z* 183.11 is consistent with loss of $[2\times CO_2+H_2]$ (Fig. 8).

$MS^3$ analysis was also performed, with fragmentation of the most abundant $MS^2$ ion at *m/z* 157.08 yielding an $MS^3$ ion at *m/z* 130.06 (see Supplementary data). This fragmentation is consistent with a loss of HCN, a pathway not feasible from the 1,2-adduct **11**.

In summary, MS and NMR studies reveal that formation of the purple chromophore observed in the *o*-ABA DHDPS assay occurs through substitution/condensation of *o*-ABA **5** with HTPA **3** to generate the diazaanthracene **12**.

### 3.4. Determination of the extinction coefficient

To determine the extinction coefficient of the purple adduct **12**, we determined the conditions under which the maximum amount of chromophore **12** was formed. The enzyme reaction time was varied from 10–40 min to deduce the time required for complete consumption of substrates (*S*)-ASA **1** and pyruvate **2** to form HTPA **3**. Purple adduct formation was initiated for each sample by quenching the enzyme reaction with acid and adding *o*-ABA **5**. The formation of adduct **12** was monitored at 540 nm by UV spectrophotometry (Fig. 3).

For each of the enzyme reaction times examined, the maximum absorbance was observed at 60 min post-addition of *o*-ABA **5**. Beyond 60 min the absorbance decreased, consistent with slow decomposition of purple adduct **12**. Maximum absorbance

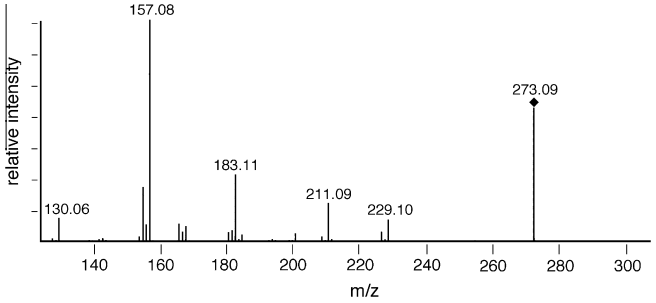


**Figure 7.** $MS^2$ analysis of parent ion at *m/z* 273.09.

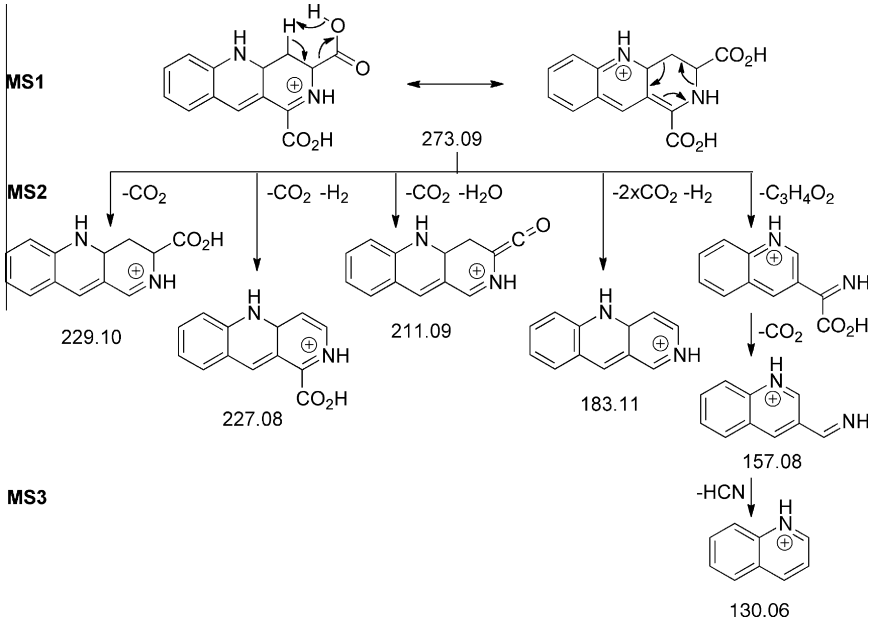


**Figure 8.** $MS^3$ fragmentation pathway via ESI-TOF-MS of adduct **12**. Mechanisms are depicted from the two resonance structures of parent compound **12** to indicate loss of $[CO_2+H_2]$ (left) and $C_3H_4O_2$ (right).

occurred after incubation of substrates **1** and **2** with DHDPS for 30 min, followed by reaction with *o*-ABA **5** and acid for 60 min. As expected, performing the enzyme reaction for only 10 min resulted in lower absorbance readings, corresponding to incomplete substrate consumption and decreased formation of HTPA **3**. Performing the enzyme incubation for 40 min resulted in a slight decrease in absorbance, consistent with degradation of HTPA **3** prior to addition of *o*-ABA **5**, suggesting that 30 min is the optimal enzyme incubation time.

Given that the maximum concentration of the purple adduct (assuming 100% conversion and no degradation) is that of the limiting substrate, (*S*)-ASA **1** (i.e., 1.0 mM), the Beer–Lambert law ($A = \varepsilon \cdot c \cdot l$) enables calculation of the extinction coefficient of the purple adduct **12** at 540 nm as $\varepsilon \geqslant 457 \pm 24\ M^{-1}\ cm^{-1}$.

## 4. Conclusions

For five decades, the chromogenic product that results when *o*-ABA **5** reacts with the product of the DHDPS-catalyzed reaction has remained a mystery. The sensitive techniques of mass spectrometry and NMR spectroscopy have now enabled determination of the identity of the purple compound as diazaanthracene **12**, which we postulate arises from stereoselective substitution of the hydroxyl group of the enamine form of HTPA **3** by the amine of *o*-ABA, with subsequent condensation with the *o*-ABA-derived aldehyde.

## Acknowledgments

This work was supported in part by the Australian Research Council (DP0770888) and the Defense Threat Reduction Agency (Project ID AB07CBT004). SRAD was funded by the Foundation for Research, Science and Technology (contract UOCX0603). The authors acknowledge Tom Hennessy from Agilent Technologies for help with LC/ESI/TOF MS analysis.

## Supplementary data

Data includes 2D NMR spectra (COSY, HSQC, HMBC), $^1H$ NMR spectrum in $H_2O$, HRMS and $MS^3$ ESI/TOF spectra, and UV–vis spectrum of **12**. Supplementary data associated with this article can be found, in the online version, at doi:10.1016/j.bmc.2010.12.029.

## References and notes

1. Lawrence, M. C.; Barbosa, J. A.; Smith, B. J.; Hall, N. E.; Pilling, P. A.; Ooi, H. C.; Marcuccio, S. M. *J. Mol. Biol.* **1997**, *266*, 381.
2. Blickling, S.; Renner, C.; Laber, B.; Pohlenz, H. D.; Holak, T. A.; Huber, R. *Biochemistry* **1997**, *36*, 24.
3. Devenish, S. R. A.; Blunt, J. W.; Gerrard, J. A. *J. Med. Chem.* **2010**, *53*, 4808.
4. Vollmer, W.; Blanot, D.; de Pedro, M. A. *FEMS Microbiol. Rev.* **2008**, *32*, 149.
5. Hutton, C. A.; Perugini, M. A.; Gerrard, J. A. *Mol. BioSyst.* **2007**, *3*, 458.
6. Hutton, C. A.; Southwood, T. J.; Turner, J. J. *Mini-Rev. Med. Chem.* **2003**, *3*, 115.
7. Cox, R. J.; Sutherland, A.; Vederas, J. C. *Bioorg. Med. Chem.* **2000**, *8*, 843.
8. Cox, R. J. *Nat. Prod. Rep.* **1996**, *13*, 29.
9. Boughton, B. A.; Griffin, M. D. W.; O'Donnell, P. A.; Dobson, R. C. J.; Perugini, M. A.; Gerrard, J. A.; Hutton, C. A. *Bioorg. Med. Chem.* **2008**, *16*, 9975.
10. Mitsakos, V.; Dobson, R. C.; Pearce, F. G.; Devenish, S. R.; Evans, G. L.; Burgess, B. R.; Perugini, M. A.; Gerrard, J. A.; Hutton, C. A. *Bioorg. Med. Chem. Lett.* **2008**, *18*, 842.
11. Dobson, R. C.; Gerrard, J. A.; Pearce, F. G. *Biochem. J.* **2004**, *377*, 757.
12. Karsten, W. E. *Biochemistry* **1997**, *36*(7), 1730.
13. Yugari, Y.; Gilvarg, C. *J. Biol. Chem.* **1965**, *240*, 4710.
14. Schöpf, C.; Steuer, H. *Justus Liebigs Ann. Chem.* **1947**, *558*, 124.
15. Schöpf, C.; Komzak, A.; Braun, F.; Jacobi, E.; Bormuth, M.-L.; Bullnheimer, M.; Hagel, I. *Justus Liebigs Ann. Chem.* **1948**, *559*, 1.
16. Vogel, H. J.; Davis, B. D. *J. Am. Chem. Soc.* **1952**, *74*, 109.
17. Larson, R. L.; Sandine, W. D.; Broquist, H. P. *J. Biol. Chem.* **1963**, *238*, 275.
18. Larson, R. L.; Broquist, H. P. *Anal. Biochem.* **1963**, *5*, 255.
19. Yamakura, F.; Ikeda, Y.; Kimura, K.; Sasakawa, T. *J. Biochem.* **1974**, *76*, 611.
20. Roberts, S. J.; Morris, J. C.; Dobson, R. C.; Gerrard, J. A. *Bioorg. Med. Chem. Lett.* **2003**, *13*, 265.
21. Pearce, F. G.; Perugini, M. A.; McKerchar, H. J.; Gerrard, J. A. *Biochem. J.* **2006**, *400*, 359.